Damage Detection in Rotorcraft Composite Structures Using Thermography and Laser-Based Ultrasound

Robert F. Anastasi[1], Joseph N. Zalameda[1], and Eric I. Madaras[2]

[1]U.S. Army Research Laboratory, Vehicle Technology Directorate, AMSRL-VT-S, Nondestructive Evaluation Sciences Branch, MS-231, NASA Langley Research Center, Hampton, VA 23681, <robert.f.anastasi@nasa.gov>, 757-864-3391

[2]NASA Langley Research Center, Nondestructive Evaluation Sciences Branch, Hampton, VA 23681

ABSTRACT

New rotorcraft structural composite designs incorporate lower structural weight, reduced manufacturing complexity, and improved threat protection. These new structural concepts require nondestructive evaluation inspection technologies that can potentially be field-portable and able to inspect complex geometries for damage or structural defects. Two candidate technologies were considered: Thermography and Laser-Based Ultrasound (Laser UT). Thermography and Laser UT have the advantage of being non-contact inspection methods, with Thermography being a full-field imaging method and Laser UT a point scanning technique. These techniques were used to inspect composite samples that contained both embedded flaws and impact damage of various size and shape. Results showed that the inspection techniques were able to detect both embedded and impact damage with varying degrees of success.

INTRODUCTION

A program titled "Survivable Affordable Repairable Airframe Program," is aimed at developing and producing new structural design concepts with lower structural weight, reduced manufacturing complexity and development time, increased readiness, and improved threat protection. This program is being conducted under the support of the U.S. Army Aviation Applied Technology Directorate (AATD) at Fort Eustis, VA, and the Rotorcraft Industry Technical Association (RITA) that included Sikorsky Aircraft Corporation, Boeing, and Bell Helicopter. Part of the program requires the demonstration and assessment of advanced field-capable nondestructive inspection (NDI) technologies to identify and characterize damage and field repairs. The potential NDI technologies should be portable, field-capable, rapid, quantitative, user-friendly, and able to inspect complex geometries. Two advanced NDI technologies; Thermography and Laser-Based Ultrasound (Laser UT), were considered. Thermography and Laser UT have the advantage of being non-contact inspection methods with Thermography being a full-field imaging method and Laser UT a point scanning technique. In this paper these technologies were used to inspect composite samples that contained both material damage and inclusions.

The advantages of thermography are noncontact, rapid inspection, single side, and imaging of large areas. In application a small amount of heat, typically less than 15 degrees Celsius above ambient, is applied to the surface of the structure. The resulting temporal temperature response can be fitted to a theoretical model for a quantitative measurement of thermal diffusivity or thickness. Thermal diffusivity is an important material property for quantitative thermal nondestructive evaluation. Changes in this material property can in part be attributed to defects [1] such as delaminations, fiber volume fraction, disbonds, matrix and fiber cracking, and gross porosity. In a thermography system, flash and quartz lamps are commonly used as heat sources. Flash lamps produce a very short duration intense pulse of heat and quartz lamps produce a long pulse of heat flux that can deliver a large amounts of energy to the sample. In general quartz lamps are more useful for inspecting thicker materials. Thermography can also be used in two different configurations, a single sided measurement where the heating and thermal detection are on one side of the sample, and through transmission where heating and detection are on opposite sides of the sample. These thermography techniques [2,3] were used used to inspect advanced composite samples and generate thermal diffusity images that show thermal condutivity changes in the samples due to material damage and inclusions.

Laser-based ultrasound is a non-contact inspection technology that uses a laser to generate ultrasound and a laser-interferometer system to measure ultrasonic surface vibrations [4,5]. The ultrasound is generated using a high-power pulsed

SEM X International Congress and Exposition on Experimental and Applied Mechanics, Costa Mesa, CA, June 2004

laser and is usually detected by a Fabry-Perot interferometer. The ultrasonic generation mechanism involves rapidly heating a small area with laser light. When the laser energy is below the material damage threshold, the mechanism is referred to as being in the thermoelastic regime, and when over this threshold, the mechanism is in the ablation regime. For nondestructive inspection the thermoelastic regime is preferred. For ultrasonic detection a continuous wave laser is typically used in conjunction with an interferometer. Light from the detection laser is scattered or reflected by the material surface and part of the light is detected and transformed by the interferometer into an ultrasonic A-scan signal that can be processed in the time and frequency domain. To generate ultrasonic C-scan or B-scan images, a series of point measurements are taken by typically scanning the laser beams over the material surface. This laser generation and detection of ultrasound is performed without mechanical contact as opposed to conventional ultrasonic techniques that require some form of mechanical contact. This non-contact nature of the technique is the prime advantage that laser-based ultrasound has over convention ultrasound.

SAMPLES

Three samples were obtained from Sikorsky Aircraft. The first sample was a flat sandwich panel with a honeycomb core, the second sample was an X-Cor™ panel and the third sample was a double ramped sandwich panel with a T-blade stiffener. During sample manufacture, inserts were embedded between composite plies or under the panel skin. The inserts were cut from a Fluorinated Ethylene Propylene (FEP) sheet that was 0.0254 mm thick. After manufacture, impact damage on these samples was created with a 2.54 cm diameter spherical impact tip at various energies. The honeycomb core sample was 61 cm by 61 cm in size. The panel skins were 2-plies of 0.2 mm plain weave graphite and were attached to each side of a 2.54 cm thick core. One-half of the sample-surface was unpainted and the other half of the surface was coated with a paint typically used in field applications. Damage conditions on each half of the panel, painted and unpainted, were the same. Thus two quadrants of the sample had identical impact damage and two quadrants had identical material inserts. The impact damage was created on the quadrants at energies of 1.0, 2.0, 3.0, and 4.0 ft-lbs. The material inserts of FEP on the quadrants had 2.54 cm and 1.27 cm round and square defects. The X-Cor™ sandwich panel was 30.5 cm by 30.5 cm in size with impact damage and pull-pin defects. The pins are attached to a face sheet skin that goes through the foam core material. Pulling or removing some of the pins created the pull-pin defects. Area of pin removal was 0.635, 1.270, 1.905, and 2.54 cm diameter. The impact damage was created using energies of 2.5, 3.5, 4.5, and 6 ft-lbs. The double ramped sandwich panel with T-blade stiffener was 50.8 cm by 96.5 cm in size and contained both inserts and impact damage defects. The surface of this panel was coated with a paint typically used in field applications. The T-blade is a stiffener on the back of the panel that runs from the panel top to bottom. The web of the T-blade is about 0.2 cm thick and has a stepped flange. A cross section of the T-blade is shown below as part of figure 5. Impact damage in the T-blade area was created with energies of 5 and 10 ft-lbs. Inserts of FEP were placed between the graphite plies to create interlaminar defects. The inserts were 2.54 cm and 1.27 cm round and square.

THERMOGRAPHY

The infrared camera used in the experimental measurements operated in the 3 to 5 micrometer wavelength range and had a cooled focal plane array. Data from the measurements were composed of a series of 16-bit digital images captured at 1/60 of a second. A PC computer was used to trigger the heat lamps and acquire the data through a data acquisition card. Thermal Imaging Analysis software developed at NASA Langley [6] was used to control the inspection parameters, store data, and perform data analysis.

Measurements and Results

Single-Sided and Through-Transmission thermal inspections were conducted on the panels. For ease of inspection the honeycomb panel was divided into 6 inspection areas, four quarters on the front surface and two quarters on the back lower surface. Each of these areas was approximately 30 cm square. A single-sided measurement of a quarter of the panel that contained impact damage was conducted. For this thermal measurement 240 frames, or 4 seconds, of data was obtained. The results in figure 1 show a visual image of the inspection area with four impact areas outlined in pencil and a thermal image where the impact areas can be seen as darker spots and some mottled areas are seen that correspond to mottled areas in the visual image. The impact energies for the four impacts were 1 ft-lb and 4 ft-lb for the top left and right and 2 ft-lb and 3 ft-lb for the bottom left and right areas respectively. The size of the thermally-detected impact-damage areas correlates with the impact energy used in creating the damage. On other quadrants of the panel, impact areas and the inserts were also detected and the painted surface did not degrade the thermal images.

A single-sided measurement of the X-Cor™ panel was conducted. For this measurement 300 frames, or 5 seconds, of data was acquired. Figure 2 shows a visual and a thermal image of the panel. In the thermal image, four dark square areas can be seen in the top half of the panel and six brighter round areas can be seen in the bottom half of the panel. The top half corresponds to impact damage where the top left spot was damaged with an impact of 6 ft-lbs, the top right area 4.5 ft-lbs, the second row left area was damaged with 3.5 ft-lbs, and the second row right area with 2.5 ft-lbs. The size of the thermally-detected impact area correlates with the impact energies, thus higher impact energy correlates to larger damage area. The individual damaged areas appear square in shape and could in part be due to the weave pattern of the composite skin. The bottom half of the panel is where the pull-pin damage is located. In each bottom left and right quadrant the smallest pull-pin area cannot be seen. The areas detected correlate with the area of the pull-pin defects. It should be noted that the thermal

image is a thermal diffusivity image that is proportional to thermal conductivity divided by the density and specific heat. The black color of the defect indicates an area of effective diffusivity conductivity, and the white area indicates increased effective thermal diffusivity. The black areas may in part include broken fibers, broken matrix, and air inclusion, while the white area may in part be due to a lack of thermal conduction into the X-Cor™ material at the pull-pin areas.

The T-blade panel was divided into three inspection areas. A single-sided inspection result is shown in figures 3 and 4 for the T-blade area. For these thermal measurements, 600 frames or 10 seconds of data was acquired. A visual image of the front surface is shown in figure 3 on the top left. This visual image shows two impact-area centers marked in white with a '+' and labeled to the right of the mark in white. The top impact-area was made with an energy of 5 ft-lb and the bottom impact-are was made with 10 ft-lb. The thermal image in figure 3 shows the impact areas circled along with enlargement of these areas. The vertical gray stripes in the thermal image correspond to the stepped flange thickness. Another thermal measurement, using the through-transmission setup, of the T-blade area is shown in figure 4. This figure shows a visual and thermal image of the damage area made with energy of 10 ft-lb and an area containing a 1.27 cm diameter insert.

LASER ULTRASOUND

Major components of the laser-based ultrasonic system include generation and detection lasers, Fabry-Perot interferometer, and optical components. Other components consist of a PC computer, oscilloscope for data acquisition, and x-y scanning bridge and controller. The generation and detection lasers in this system are both Nd:YAG lasers. The generation laser is a Q-switched pulsed laser with a wavelength of 1064 nm, and has variable pulse energy up to 200 mJ with pulse duration of 20 nsec. This pulse width produces ultrasound with a center frequency of about 5 MHz. The detection laser is a continuous wave laser with a wavelength of 532 nm, beam diameter of 0.32 mm, maximum output power of 400 mW, and a line stability of less then 10 kHz. The light from the lasers and light traveling from the material under inspection to the interferometer are completely contained within, 60-foot fiber optic cables that run from the lasers on the optical table to the lenses on the scanning bridge. Light from the generation laser travels through the fiber optic cable to a lens on the x-y scanning bridge. This lens focuses the laser light onto the surface of the material being inspected. The generation laser pulse creates ultrasonic waves that travel in the material being inspected. Light from the detection laser travels through the fiber optic cable to a second lens on the x-y scanning bridge. This second lens focuses the laser light onto the surface of the sample being inspected. This light is reflected and scattered from the surface. Part of the reflected and scattered light is collected by a third lens, on the x-y scanning bridge, that transmits the light to the Fabry-Perot Interferometer via fiber optic cable. The distance between the lenses on the x-y scanning bridge and the material under inspection is approximately 25 cm. A PC-based virtual instrument controls the scanning stage and stores the ultrasonic signals for later processing. This system has been used to inspect thick stitched composite material for damage [7].

Measurements and Results

The specimens tested with laser UT included the sandwich honeycomb panel, the T-blade panel, and a scrap piece of woven graphite sample that was used to evaluate the laser-material damage threshold. Damage thresholds tests were conducted on the bare surface of a woven-graphite sample and the black surface of the honeycomb panel. As noted earlier, the lasers used in this system are both Nd:YAG lasers. The generation laser is a pulsed laser with a wavelength of 1064 nm and the detection laser is a continuous wave laser with a wavelength of 532 nm. Generation laser tests on the 6-ply woven graphite sample showed the threshold of damage to be between 10 and 15 mJ/pulse with a 5 mm diameter spot size. The damage appears as a dull spot on a shiny surface, but on closer inspection the surface itself doesn't appear damaged. It is possible the matrix material may be transparent to the laser generation wavelength and thus the fibers are directly heated, expand, and de-bond from the matrix material and the crazing between the fiber and matrix material makes the damage area appear less glossy. Similar tests on a painted section of the honeycomb core panel showed the threshold of damage at approximately the same level as on the bare graphite sample. Laser pulse energies of 1, 2, 5, and 10 mJ/pulse were used to test for damage. The appearance of damage on the painted surface became questionable at the 10 mJ/pulse level when a very slight discoloration in the surface could be seen. This slight surface discoloration was acceptable damage and thus laser pulse energy of 10mJ/pulse was used in the measurements. Detection laser tests on both samples showed no visible damage for a power of 150 Watts with a 2 mm-diameter laser beam that was incident on the sample for a few seconds.

An area of the sandwich honeycomb core panel was prepared for laser-based ultrasonic inspection by applying a thin layer of vacuum grease in about a 7.6 cm square area around an impact site. The vacuum grease enhances the generation of ultrasound for the 1064 nm wavelength, by acting as a constraining layer. Enhancements of around 25 dB were demonstrated with the application of light oil [4]. The vacuum grease also acted as a reflective coating for the 532 nm wavelength and thus provided more light for the interferometer measurement. A series of points were inspected across an impact area. The ultrasonic signature from these points across the inspection area did not show major variations as would be expected from delaminations occurring in the outer skin. This could in part be due to damage being near the front surface and the ultrasonic reflections being obscured by the initial impulse from the laser. No further measurements were made on the honeycomb panel.

The T-blade panel was inspected across the T-blade area with laser UT. The first area inspected was around the 10 ft-lb impact site. The area scanned was 8.9 cm wide by 6.4 cm in height with 0.254 cm increments between inspection points. The ultrasonic waveforms were processed to generate a time-of-flight C-scan image. In cases were the amplitude of the back wall

echo was not clear, a time-of-flight between the main bang and back-wall echo was assigned a value of zero. Figure 5 shows the T-blade profile and the time-of-flight C-scan. Thickness changes in the T-blade correspond to color changes in the C-scan. An ultrasonic signal loss was observed for the web/fillet area of the T-blade and is seen as a vertical strip in the center of the scan area. In the center of the scan is a circular area, approximately 1.9 cm wide by 1.0 cm high. This is the damage area around the 10 ft-lb impact. Additional sections were scanned with the same dimensions and incremental spacing. The processed images were then pasted together to form a composite image. This composite image included the 10 ft-lb impact and the area below it, almost to the edge of the sample. The composite C-scan is shown in figure 6 and covers an area 8.9 cm wide by 22.8 cm high. This image shows the loss of echo in the T-blade web area, the 10 ft-lb impact, and two embedded defects. The embedded defects are 1.27 cm in diameter and 0.65 cm in diameter. This C-scan images shows that the general structure in the T-blade and that it was possible to observe a 0.025 cm thickness changes in this structure. Material inserts could be detected, but inserts near the flange were partially obscured. The impact damage area for the 10 ft-lb site was readily seen, but partially obscured due to the flange.

DISCUSSION

NDI technologies of Thermography and Laser UT were used to inspect composite panels for defects that included material damage and material inserts. Thermography measurements were conducted on the three panels using both single-sided and through-transmission methods. Thermography was successful in detecting most of the material defects and inserts. For the composite honeycomb panel, the smallest impact damage defect was barely detectable and could have been missed in a blind study, but all other defects were detected. The panel painted surface did not adversely effect the thermal inspection, but seemed to enhance the damage detection. Laser UT C-scan results were most promising on the T-blade panel in the T-blade area, but not on the honeycomb panel and which could be due in part to the thinness of the panel skins. The C-scan images along the T-blade showed the 10 ft-lb impact damage, and the embedded defects. These images also showed that the general structure of the T-blade could be seen and that it was possible to observe 0.025 cm thickness changes in the structure. In general the laser-based ultrasound appears to be a viable method for inspecting the T-blade for thickness variations and more extensive impact damage. The results show Thermography to be better at detecting damage and material inclusions in the honeycomb and X-Cor™ panels and not as well at detecting the damage in the T-blade area. The opposite of this is the case for Laser UT. It did not do well on the honeycomb panel, but did a good job in the T-blade area. Thus the two methods compliment each other.

ACKNOWLEDGMENT

This research was supported and partially funded by Sikorsky Aircraft Corporation, Stratford, CT and the U.S. Army Aviation Applied Technology Directorate, Fort Eustis, VA under Technology Investment Agreement No. DAAH10-02-2-0001.

REFERENCES

1. Winfree, W.P., Heath, D.M., “Thermal Diffusivity Imaging of Aerospace Materials and Structures,” Thermosense XX, edited by J.R. Snell and R.N. Wurzbach, SPIE Proceedings Vol. 3361, Bellingham, WA, pp. 282-290, 1998.
2. Zalameda, J.N. and Winfree W.P., "Quantitative Thermal Nondestructive Evaluation Using an Uncooled Microbolometer Infrared Camera,” Proceedings of SPIE, Vol. 4710, pp. 610-617, April 1-5, 2002.
3. Zalameda J.N., Farley G.L., and Smith, B.T., “A Field Deployable Nondestructive Impact Damage Assessment Methodology for Composite Structures,” American Society for Testing and Materials Journal of Composites Technology and Research, Vol. 16, No. 2, pp 161-169, April 1994.
4. Scruby, C.B. and Drain, L.E., “Laser Ultrasonics: Techniques and Applications,” Adam Hilger, New York, 1990.
5. Hutchins, D.A., “Ultrasonic Generation by Pulsed Lasers,” Physical Acoustics. Vol. 18, 1988.
6. Cramer, K.E. and Syed, H.I., “TIA Software User's Manual,” NASA TM-4687, September 1995.
7. Anastasi, R.F., Friedman, A.D., Hinders, M.K., and Madaras, E.I., "NDE of Damage in Thick Stitched Composites Using Laser-Based Ultrasound with Optical Fibers," Materials Evaluation, Vol. 56, No. 12, December 1998.

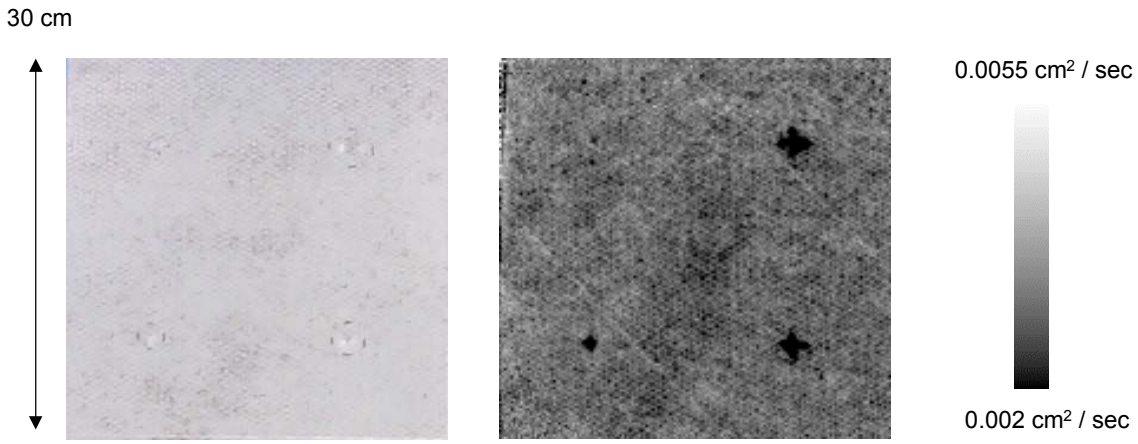

Figure 1. Visual (left) and thermal diffusivity inspection image (right) are area I of the honeycomb panel.

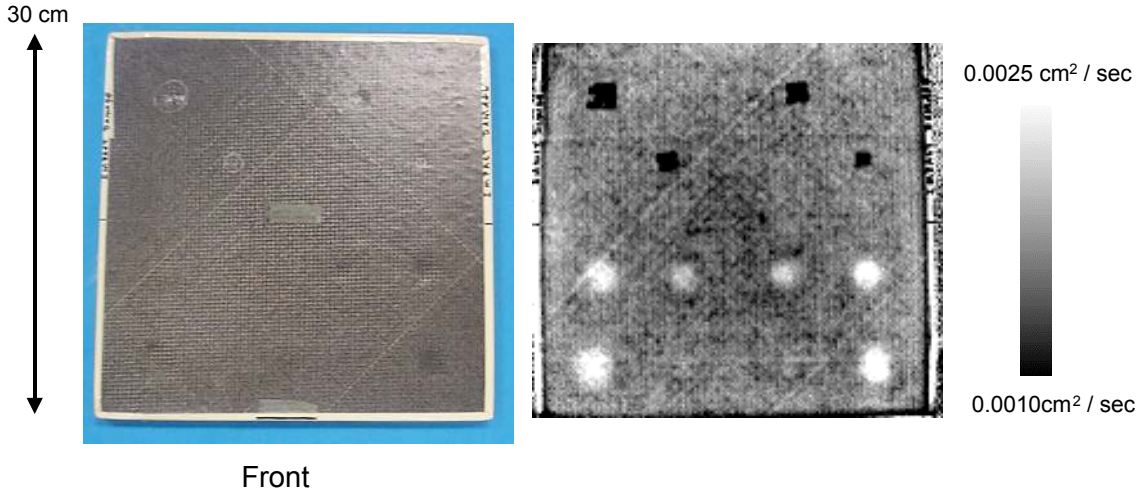

Figure 2. Visual (left) and thermal diffusivity inspection image (right) are the front side of X-Cor™ panel.

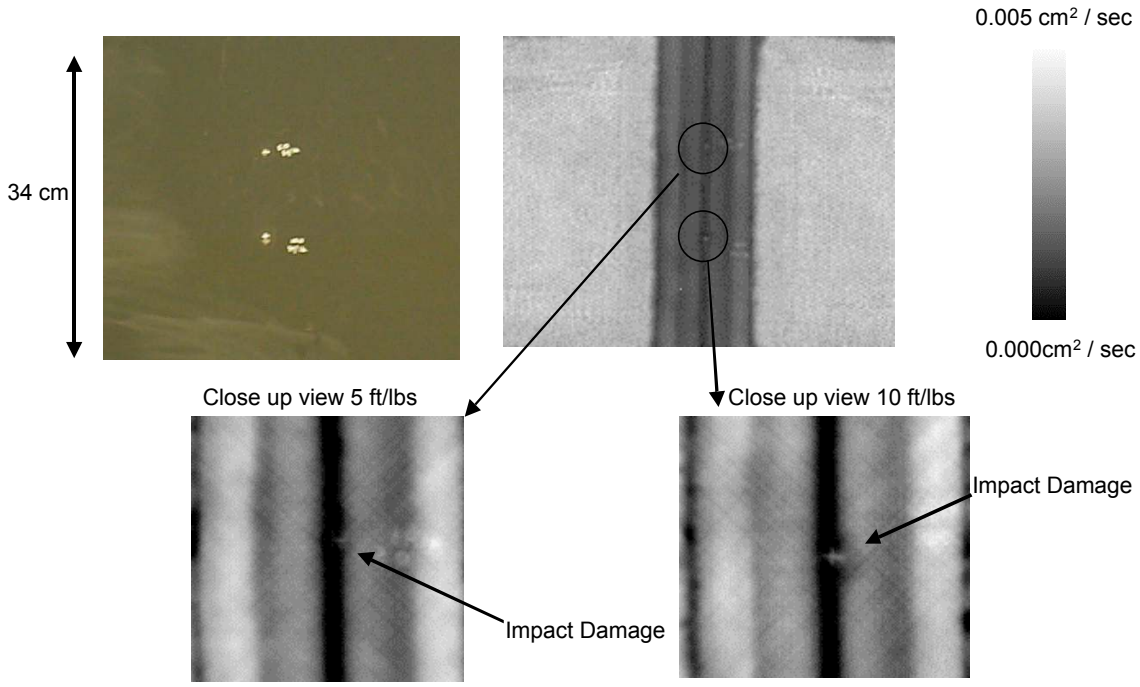

Figure 3. Visual (left-top) and thermal diffusivity inspection image (top-rigth and bottom) show the T-blade area and close up views of the 5 ft-lb and 10 ft-lb impacts.

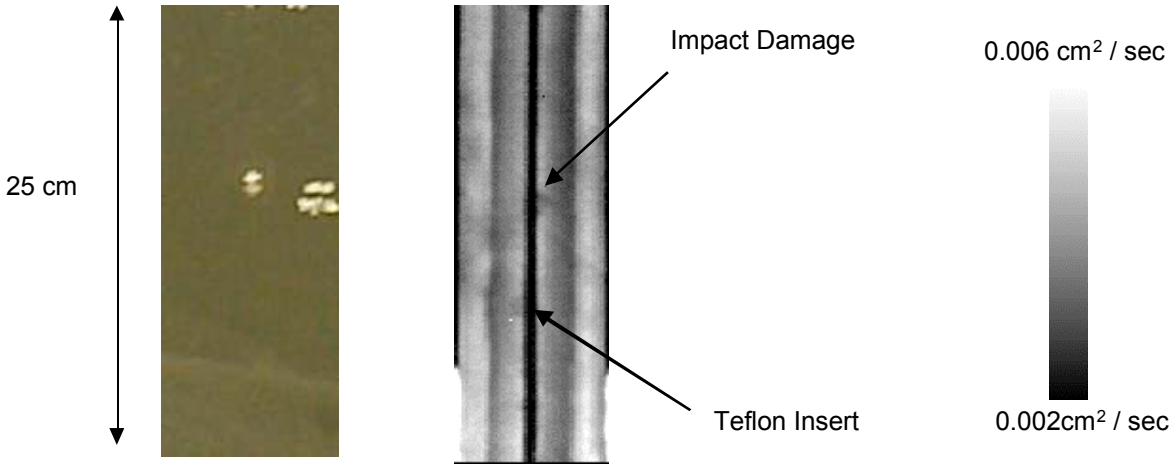

Figure 4. Visual (left) and thermal diffusivity inspection image (right) show the T-blade area and includes the 10 ft-lb impact area and material insert.

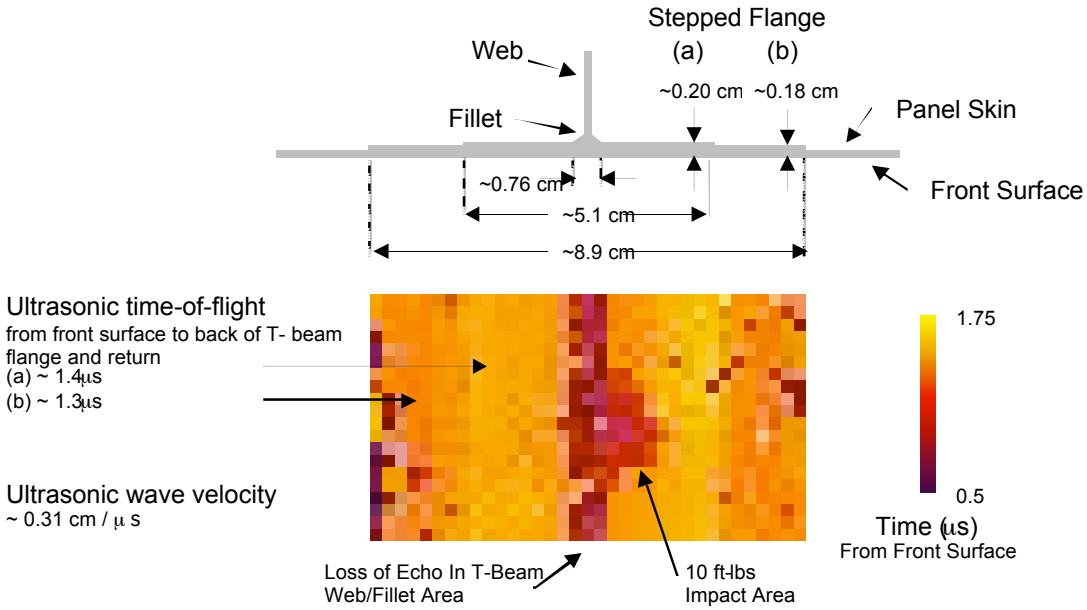

Figure 5. T-blade profile and time-of-flight C-scan around the 10 ft-lb impact site.

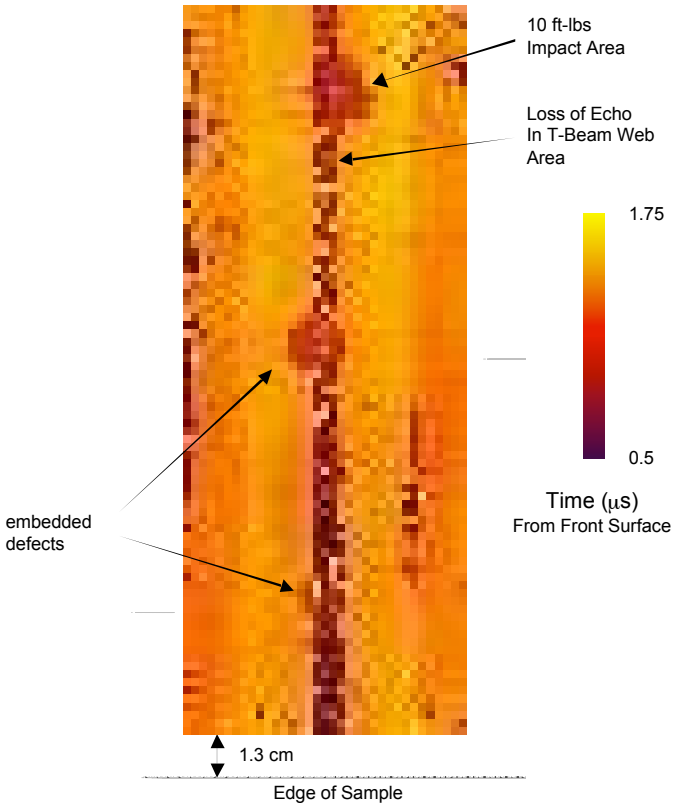

Figure 6. Time-of-flight C-scan image showing the loss of echo in the T-blade web area, the 10 ft-lb impact, and two embedded defects. The scan area is 8.9 x 22.9 centimeters.